Microwave Backscattering from Oil-Covered Sea Surface with Two-Scale Model

Chao Yang[1], * and Lixin Guo[2]

Abstract—The electromagnetic scattering from oil-covered sea surface is investigated by two scale model with the help of Lombardini's oil-covered sea spectrum and the semi-empirical reflection model that takes the oil film into consideration. Firstly, a comparison of the clean and oil-covered sea spectra is made to show the influence of the oil film on the sea surface. Then, the backscattering coefficient from the clean sea computed by the two scale model is compared with the measured data in the reference to validate the accuracy of the two scale model used in this paper. Finally, backscattering features from the oil-covered sea surface are discussed in detail and compared with those from the clean sea. In addition, the influence of the thickness of oil film and fractional filling factor on the backscattering coefficient of oil-covered sea are also studied. The simulated results show that the oil film floating on the sea has remarkable influence on the backscattering coefficient of the sea, compared with those of the backscattering coefficient from the clean sea.

1. INTRODUCTION

Investigation of the electromagnetic scattering from the rough sea surface is an active research topic, with applications in the fields of sea state surveillance, target recognition, maritime communication system, remote sensing of ocean, etc. [1–3]. In recent years, many researchers have paid their attention to the problem of electromagnetic scattering from oil-polluted sea surface [4–8] mainly caused by oil spill accident and biogenic slicks due to the study of the electromagnetic scattering from the oil-covered sea, which has significance in the field of oil spill surveillance and ocean remote sensing [9, 10]. It is well known that two major methods, including asymptotic method [1] and numerical method, are commonly used for calculating the scattering features of sea surface. The asymptotic method includes the small perturbation method (SPM), Kirchhoff approximation (KA), two-scale model (TSM) [11, 12], and small slope approximation (SSA) [13]. The SPM is valid for small scale surface, whereas the KA is suitable for large scale surface. The TSM and SSA are good alternatives to bridge the gap between the SPM and KA. The numerical method contains the method of moment (MOM) [14], finite-difference time-domain (FDTD) [15], etc., which can obtain exact scattering features according to the electromagnetic theory. However, although the numerical method has the advantage of high accuracy, it also has the drawback of large computation compared with that of the asymptotic method. Zamani et al. [16] derived the perturbative solution of multilayered rough surfaces and computed the cross-polarized scattering features from them. Iodice et al. [17] discussed the scattering from both fractal and classical rough surfaces under the Kirchhoff approximation, and the physical interpretation was also given. Wu et al. [18] analyzed the scattering coefficient from dynamic ocean surface with a two-scale model, and the effect of the model parameters on the scattering coefficient was discussed in detail. Li et al. [19] utilized

the small slope approximation method to predict the normalized radar cross section of electrically large rough sea surface.

In this work, the TSM is adopted to compute scattering features from the oil-covered sea surface since it can simultaneously take merits of both SPM and KA into consideration and broaden the range of validity of the SPM and KA. More importantly, a comparison investigation between the clean sea and oil-covered sea is made to examine the effect of oil film on the sea surface scattering features. In addition, the influence of oil film parameters on sea surface scattering coefficient is also studied.

2. THE OIL-COVERED SEA SPECTRUM

In order to investigate the electromagnetic scattering from the oil-covered sea surface, the oil-covered sea spectrum should be firstly given. In this paper, the oil-covered sea spectrum is constructed via the clean sea spectrum and Lombardini's damping coefficient. The semi-empirical sea spectrum $W(k)$ is described by [20]

$$W(k) = \begin{cases} \dfrac{a}{k^3} \exp\left(\dfrac{-0.74 g^2}{k^2 u_{19.5}^4}\right) & k < 0.04\,\text{rad/cm} \\[3mm] 0.875(2\pi)^{p-1}\left(1 + \dfrac{3k^2}{k_m^2}\right) \times g^{(1-p)/2}\left[k\left(1 + \dfrac{k^2}{k_m^2}\right)\right]^{-(p+1)/2} & k > 0.04\,\text{rad/cm} \end{cases} \tag{1}$$

where a is 1.4×10^{-3}; k_m is $3.63\,\text{rad/m}$; the gravitational acceleration g is $981\,\text{cm/s}^2$; $p = 5 - \log_{10}(u_f)$. The relation between the friction velocity u_f and windspeed $u(z)$ at an altitude of z is given by

$$u(z) = (u_f/0.4)\ln\left(\frac{z}{0.684/u_f + 4.28 \times 10^{-5}u_f^2 - 0.0443}\right)\,\text{cm/s} \tag{2}$$

Based on the semi-empirical sea spectrum model, the one-dimensional oil-covered sea spectrum model $W_c(k)$ can be expressed as follows [4, 21]

$$W_c(k) = W(k)/(1 - F + F/y_D) \tag{3}$$

where F is the fractional filling factor used to deal with the partially oil-covered sea surface, and y_D is the Lombardini's damping attenuation coefficient, for the insoluble oil film, and given by

$$y_D(f, E_0, \omega_D) = \frac{1 - 2\tau + 2\tau^2 - X + Y(X + \tau)}{1 - 2\tau + 2\tau^2 - 2X + 2X^2} \tag{4}$$

where

$$\tau = \sqrt{\omega_D/2\omega} \quad X = \frac{E_0 k^2}{\rho(2\eta\omega^3)^{1/2}} \quad Y = \frac{E_0 k}{4\eta\rho\omega}$$

are dimensionless quantities and

$$f = \frac{\omega}{2\pi} = \frac{(\varsigma k^3/\rho + gk)^{1/2}}{2\pi} \tag{5}$$

Equation (5) is the dispersion law; f is the frequency; ω is the angular frequency; E_0 is the elasticity modulus; the water density is $\rho = 10^3\,\text{kg/m}^3$; the kinematic viscosity is $\eta = 10^{-6}\,\text{m/s}^2$; the surface tension is $\varsigma = 74 \times 10^{-3}\,\text{N/m}$; and ω_D stands for the characteristic pulsation.

In order to account for the unidirectional effect due to the wind direction, the corresponding two-dimensional sea spectrum is written as

$$W_c(k, \phi) = W_c(k)[a_0 + a_1(1 - \exp(-bk^2))\cos 2\phi] \tag{6}$$

where a_0 and b are constants taken as $1/2\pi$ and $1.5\,\text{cm}^2$, respectively. ϕ stands for the wave beam direction relative to the wind direction. The value of a_1 should refer to [20] and be modified when the oil-covered sea is concerned with.

3. THE TWO-SCALE MODEL FOR THE OIL-COVERED SEA SURFACE

In the framework of the TSM, the rough sea surface is usually divided into small and large roughness, and the SPM is valid for the small roughness surface, while the KA is accurate for the large roughness surface. The TSM is a combination of SPM and KA, and the SPM is adopted to calculate the scattering coefficient from the small roughness surface, and taking average with respect to the scattering coefficient over the slope distribution of the large scale roughness to consider the tilting effect of the large roughness surface. In order to take the shadow effect and the curvature effect in the SPM model into account, the backscattering coefficients of the TSM for different incident angles and azimuth angles are expressed as [1, 22]

$$\sigma_{hh}(\theta_i, \varphi) = S(\nu) \int_{-\infty}^{\infty} \int_{-\cot\theta_i}^{\infty} \left(\hat{h} \cdot \hat{h}'\right) c_{hh}\left(\theta_i', k, R\right) \times \sigma_{hh}'\left(\theta_i', \varphi\right)(1 + z_x \tan\theta_i) P\left(z_x, z_y\right) dz_x dz_y \quad (7)$$

$$\sigma_{vv}(\theta_i, \varphi) = S(\nu) \int_{-\infty}^{\infty} \int_{-\cot\theta_i}^{\infty} \left(\hat{v} \cdot \hat{v}'\right) c_{vv}\left(\theta_i', k, R\right) \times \sigma_{vv}'\left(\theta_i', \varphi\right)(1 + z_x \tan\theta_i) P(z_x, z_y) dz_x dz_y \quad (8)$$

where $\hat{h}$ and $\hat{v}$ are the unit vectors of horizontal and vertical polarizations in the primed coordinate, respectively. Similarly, $\hat{h}'$ and $\hat{v}'$ are the corresponding unit vectors in the local coordinate. θ_i and θ_i' are the incident angles in the primed and local coordinates, respectively. φ is the rotation angle between the primed and local coordinates. $z(x, y)$ denotes the height distribution of rough surface, and z_x and z_y are the surface slopes along the x and y-axes in the primed coordinate, respectively. $P(z_x, z_y)$ is the large scale roughness slope probability density function provided by Cox and Munk [23]. $\sigma_{hh}'(\theta_i')$ and $\sigma_{vv}'(\theta_i')$ are the backscattering coefficient of the SPM model over the small scale roughness surface in the local coordinate, which are given by [1]

$$\sigma_{hh}'\left(\theta_i', \varphi\right) = 8k^4 \cos^4\theta_i' |\alpha_{hh}|^2 W\left(2k\sin\theta', \varphi\right) \quad (9)$$

$$\sigma_{vv}'\left(\theta_i', \varphi\right) = 8k^4 \cos^4\theta_i' |\alpha_{vv}|^2 W\left(2k\sin\theta', \varphi\right) \quad (10)$$

where k is the wavenumber. The field coefficients α_{hh} and α_{vv} depend on the incident angle and dielectric constant, and the detailed information about them can be found in [1].

In order to compute the scattering coefficient from the oil-covered sea surface, a semi-empirical sea spectrum model with the oil film [4, 6] taken into consideration that treats the oil layer floating on the clean sea as upper air-oil interface and lower oil-sea interface by replacing the Fresnel reflection coefficient $r_{12}(\chi_i)$ at air-oil interface with the equivalent Fresnel reflection coefficient $r_{eq}(\chi_i)$, and the equivalent Fresnel reflection coefficient $r_{eq}(\chi_i)$ can be obtained as [4]

$$r_{eq}(\chi_i) = \frac{r_{12}(\chi_i) + r_{23}(\chi_m)e^{-j\Delta\phi}}{1 + r_{12}(\chi_i)r_{23}(\chi_m)e^{-j\Delta\phi}} \quad (11)$$

where $r_{23}(\chi_i)$ is the Fresnel reflection coefficient at oil-sea interface; $\chi_i = -(\theta_s - \theta_i)/2$ is defined as the local incident angle; θ_s is the scattering angle; $\Delta\phi = 2k_2 H \cos\chi_m$ is the phase difference; χ_m is the angle of refraction; H is the thickness of oil film; and k_2 is the wavenumber inside the oil film.

Finally, the two scale model for the oil-covered sea surface is presented as

$$\sigma^{sc} = \left|\frac{r_{eq}(\chi_i)}{r_{12}(\chi_i)}\right|^2 \sigma^{\text{air/oil}} \quad (12)$$

where $\sigma^{\text{air/oil}}$ stands for the scattering coefficient from the air-oil interface calculated with Equations (7) and (8).

4. NUMERICAL RESULTS

The sea spectrum has crucial importance for describing the variation of the sea surface. Initially, a comparison of one dimension sea spectrum between the clean sea and the oil-covered one is shown in Fig. 1. The variation of sea spectrum with wavenumber is given. The friction velocity is $12\,\text{cm/s}$, two types of parameters for the oil-covered sea surface are ($E_0 = 9\,\text{mN/m}$, $\omega_D = 6\,\text{rad/s}$) and
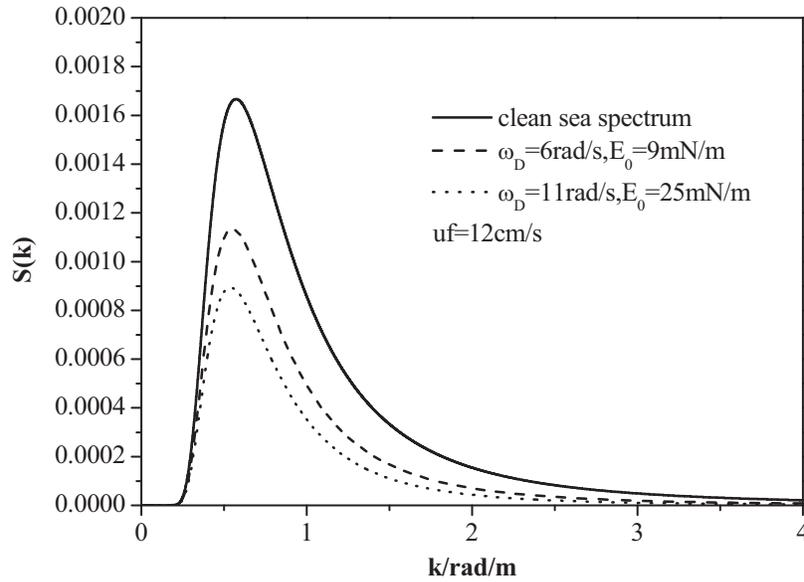
Figure 1. The comparison of the sea spectrum versus wavenumber for clean and oil-covered sea.
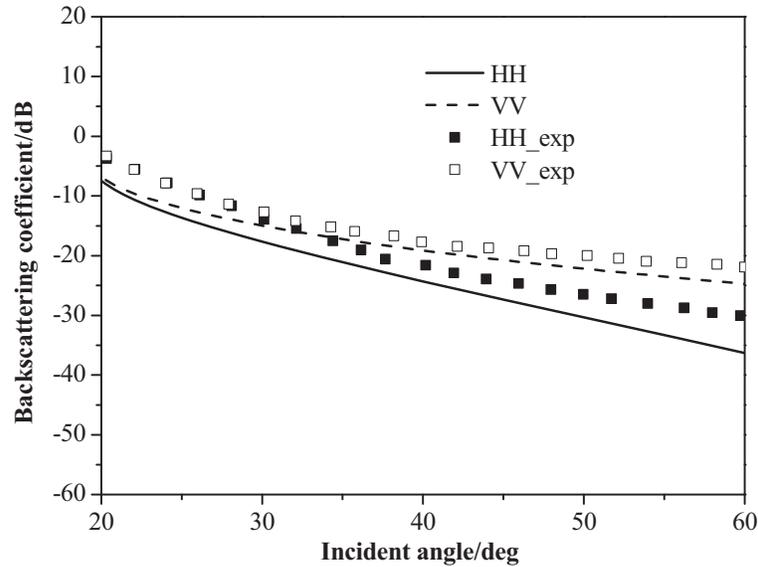
Figure 2. The comparison of the backscattering coefficient of the clean sea with the experimental data.

($E_0 = 25\,\text{mN/m}$, $\omega_D = 11\,\text{rad/s}$). One can observe that damping phenomena can be clearly seen from Fig. 1 with the increase of the wavenumber, and all spectrum peaks move to the region of small wavenumber because of the existence of the oil film floating on the sea.

Then, the TSM with the semi-empirical reflection model taken into consideration is utilized to discuss the scattering coefficient from the oil-covered sea surface. The backscattering coefficient of the clean sea surface with TSM model is tested with the experimental data [13], which is shown in Fig. 2. The simulation parameters are identical to [13]. The radar working frequency is 14.019 GHz. The windspeed at an altitude of 10 m above the mean sea level is 5 m/s. The relative dielectric constant of the sea water is $(32.35, -36.6)$, and the $\varphi = 0.0$ means that the simulation is carried out in the upwind direction. It is clearly demonstrated that the backscattering coefficient decreases as the incident angle increases, and the backscattering coefficient for VV polarization is a little bigger than that of HH polarization case,

especially for large incident angle. The simulation results are somewhat underestimated for both HH and VV polarizations. Nonetheless, the simulation results computed by TSM are essentially in good agreement with the experimental data for both HH and VV polarizations.

Next, much attention is paid to the influence of the oil film floating on the sea surface on backscattering coefficient. Fig. 3 displays the comparison of the change of the backscattering coefficient with the azimuth angle between the clean and oil-covered sea surfaces for HH and VV polarizations. The radar working frequency is 3 GHz. The windspeed at an altitude of 10 m above the mean sea level is 5 m/s. The relative dielectric constant of the sea water is $(70.4, -40.6)$. The relative dielectric constant of the oil is $(2.25, -0.01)$. The thickness of oil film is 10 mm. The incident angle is $45°$. The parameters
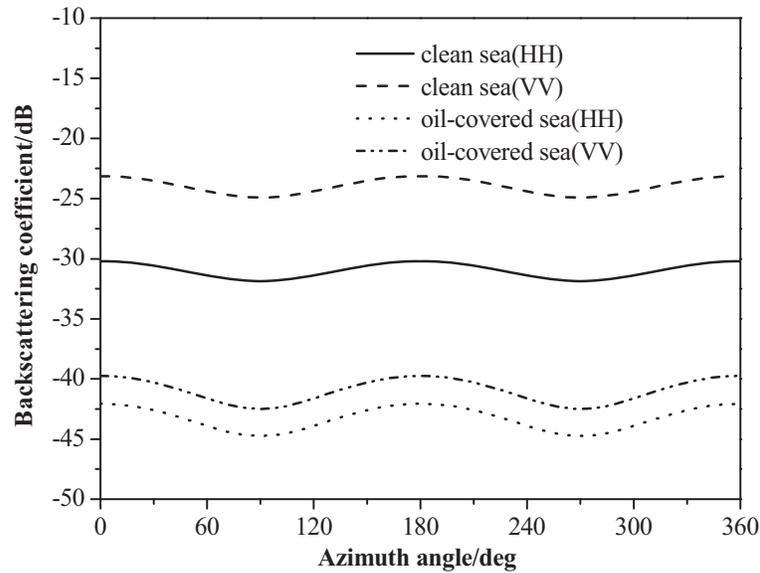
Figure 3. The comparison of the backscattering coefficient versus azimuth angle between the clean and oil-covered sea surface.
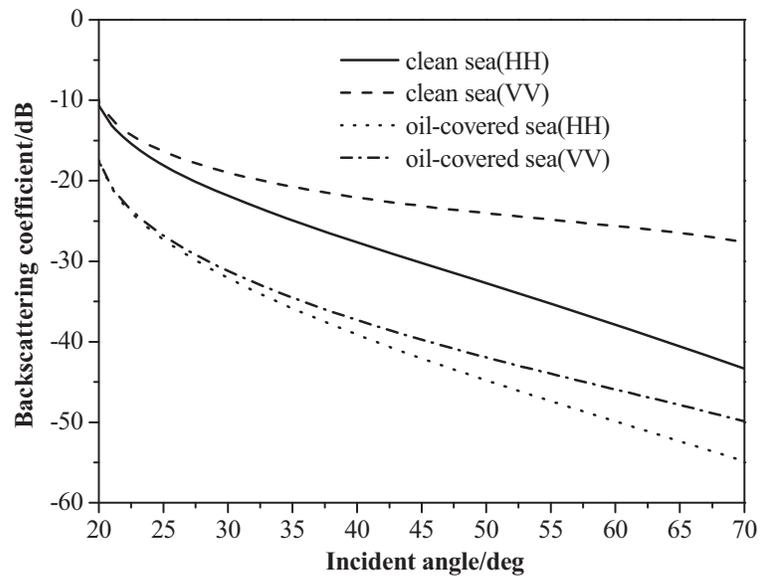
Figure 4. The comparison of the backscattering coefficient versus incident angle between the clean and oil-covered sea surface.

for the oil-covered sea surface are ($E_0 = 9\,\text{mN/m}$, $\omega_D = 6\,\text{rad/s}$). The fractional filling factor $F = 1.0$, which means that a fully oil-covered sea is considered, and the backscattering coefficient is discussed in the upwind direction. From Fig. 3, the periodic variation in the backscattering coefficient versus azimuth angle for clean sea and oil-covered sea is obviously exhibited, and the backscattering coefficients of VV polarization for the two cases are distinctly greater than those of the HH polarization. In addition, for both HH and VV polarizations, the backscattering coefficients versus the azimuth angle for the clean sea are obviously higher than those of the oil-covered sea, which may be due to the oil film floating on the sea surface. On the one hand, it can exert the damping effect on the sea spectrum and reduce the sea surface roughness, that is to say, the oil film makes the sea surface smooth. On the other hand, the relative dielectric constant of the oil film can also affect the backscattering coefficient.

Since the radar backscattering coefficient is an important research aspect in the field of ocean remote sensing, the comparison of the backscattering coefficient versus incident angle between the clean
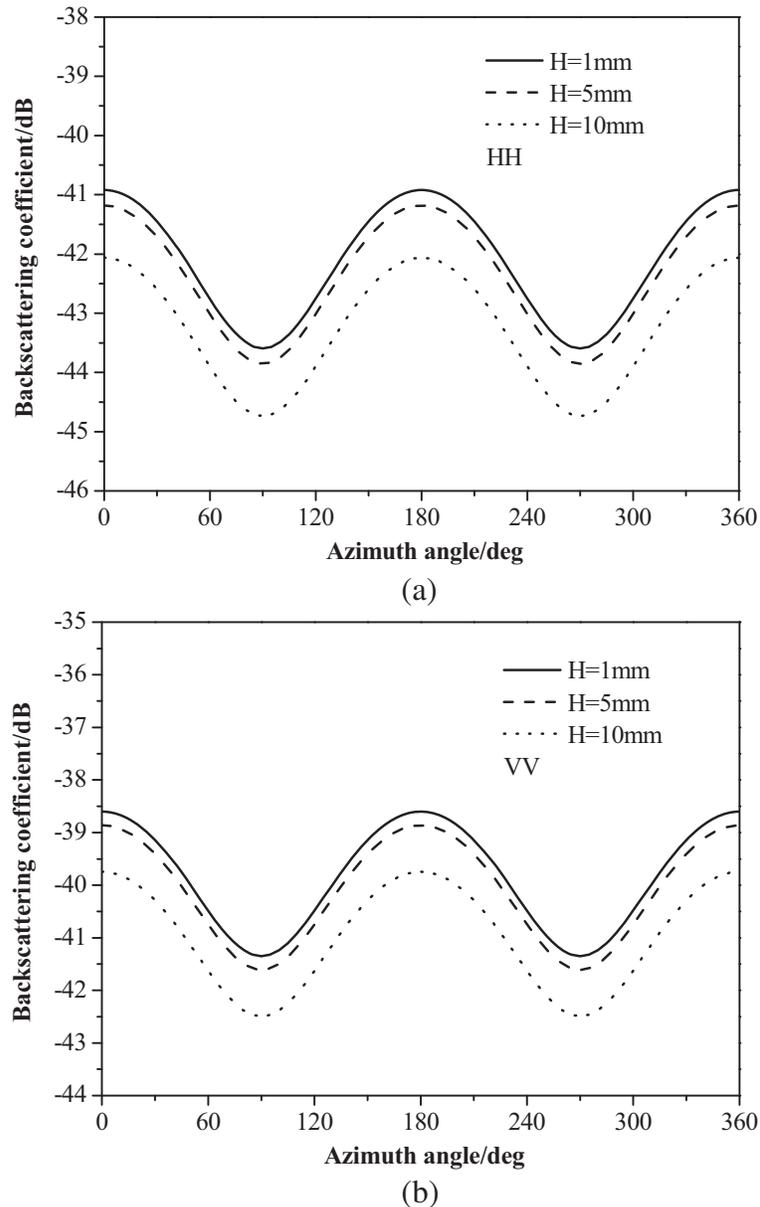
Figure 5. The influence of the thickness of oil film on the backscattering coefficient versus azimuth angle: (a) HH polarization; (b) VV polarization.

and oil-covered sea surface is illustrated in Fig. 4. In the subsequent discussion, it should be noted that the parameters are the same as those of Fig. 3 except for the special instructions. It can be seen that the clean sea backscattering coefficients with respect to all incident angle for both HH and VV polarizations are also significantly greater than those of the oil-covered sea. The reason is the same as those explained in Fig. 3.

To further investigate the influence of the thickness of oil film on the backscattering coefficient from oil-covered sea surface, the curves of backscattering coefficient versus azimuth angle with different thicknesses of oil film are demonstrated in Fig. 5. It is readily seen that the backscattering coefficient decreases with the increase of the thickness of oil film for all azimuth angles for both HH and VV polarizations. It seems to be easily explained by the fact that the damping effect is enhanced as the thickness of oil film increases, that is to say, the thicker the oil film, the smoother the sea surface.

(a)

(b)
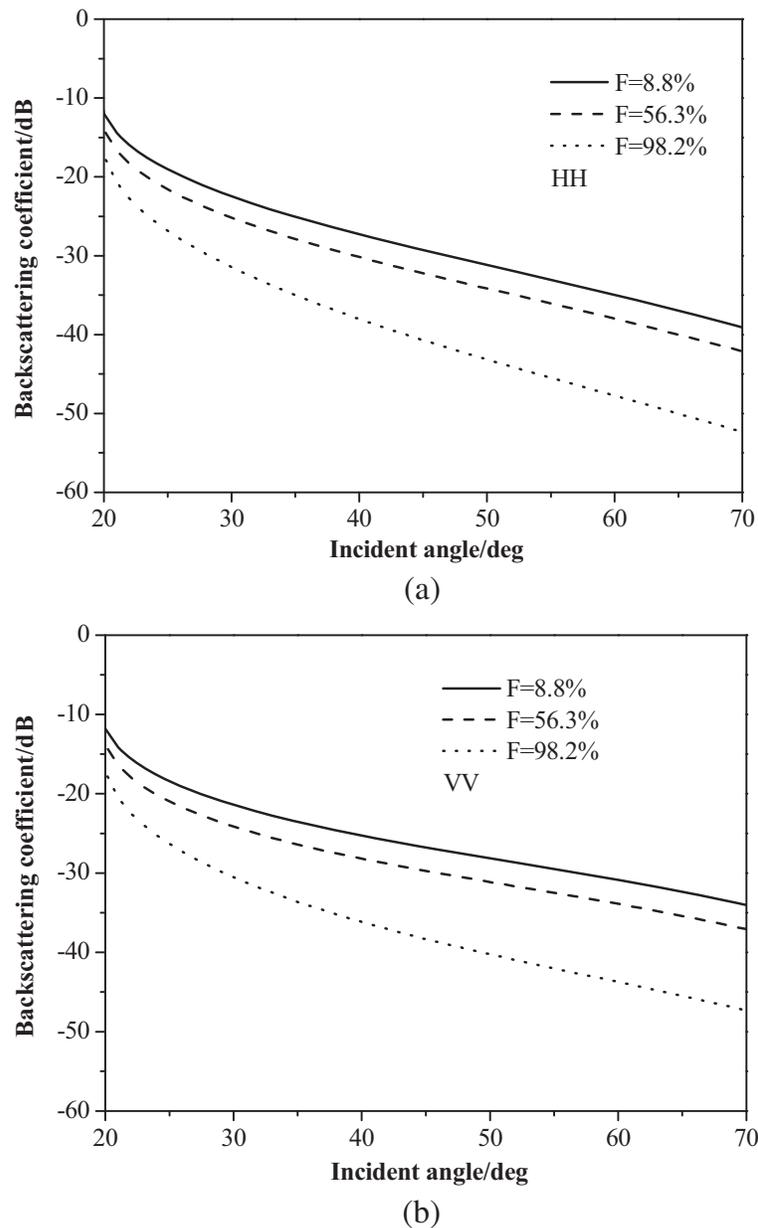
Figure 6. The influence of fractional filling factor on the backscattering coefficient versus incident angle: (a) HH polarization; (b) VV polarization.

It should be noted that only backscattering features of a fully oil-covered sea surface are analyzed in the above discussion. Furthermore, backscattering features of a partial oil-covered sea surface are also investigated, and the partial oil-covered sea surface is embodied by the fractional filling factor F in Equation (3). Fig. 6 demonstrates the influence of fractional filling factor on the backscattering coefficient versus incident angle, and it can be observed that the backscattering coefficient from the partial oil-covered sea surface increases as the fractional filling factor F decreases for both HH and VV polarizations. This is mainly because the damping effect of the oil film on the sea surface is weakened as the fractional filling factor F decreases, and when $F = 0$, a partial oil-covered sea surface is transformed into a clean sea surface.

5. CONCLUSION

In this paper, two scale method combined with the semi-empirical equivalent reflection model is presented to simulate backscattering features from the oil-covered sea surface, and the backscattering coefficients from oil-covered sea surface are compared with those of the clean one. In addition, the influences of parameters such as the thickness of the oil film and fractional filling factor, which are utilized to describe the oil-covered sea, on the backscattering coefficient are also investigated. The results show that the oil film has noticeable impact on electromagnetic scattering features. Therefore, it is potentially of great significance for the field of oil spill surveillance.

ACKNOWLEDGMENT

REFERENCES

1. Ulaby, F. T., R. K. Moore, and A. K. Fung, *Microwave Remote Sensing: Active and Passive. Vol. II. Radar Remote Sensing and Surface Scattering and Emission Theory*, Addison-Wesley, New Jersey, NJ, 1982.
2. Ishimaru, A., *Wave Propagation and Scattering in Random Media*, Academic Press, New York, NY, 1978.
3. Yang, C., W. Jin, and L.-X. Guo, "Electromagnetic wave propagation over oil-covered sea surface," *Chinese Physics Letters*, Vol. 29, No. 7, 074210, 2012.
4. Pinel, N., N. Dechamps, and C. Bourlier, "Modeling of the bistatic electromagnetic scattering from sea surfaces covered in oil for microwave applications," *IEEE Transactions on Geoscience and Remote Sensing*, Vol. 46, No. 2, 385–392, 2008.
5. Nunziata, F., P. Sobieski, and M. Migliaccio, "The two-scale BPM scattering model for sea biogenic slicks contrast," *IEEE Transactions on Geoscience and Remote Sensing*, Vol. 47, No. 7, 1949–1956, 2009.
6. Pinel, N., C. Bourlier, and I. Sergievskaya, "Two-dimensional radar backscattering modeling of oil slicks at sea based on the model of local balance: Validation of two asymptotic techniques for thick films," *IEEE Transactions on Geoscience and Remote Sensing*, Vol. 52, No. 5, 2326–2338, 2014.
7. Montuori, A., F. Nunziata, M. Migliaccio, and P. Sobieski, "X-band two-scale sea surface scattering model to predict the contrast due to an oil slick," *IEEE Journal of Selected Topics in Applied Earth Observations and Remote Sensing*, Vol. 9, No. 11, 4970–4978, 2016.
8. Wang, R., L. Guo, and Z. Zhang, "Scattering from contaminated rough sea surface by iterative physical optics model," *IEEE Geoscience and Remote Sensing Letters*, Vol. 13, No. 4, 500–504, 2016.
9. Fingas, M. and C. Brown, "Review of oil spill remote sensing," *Spill Science & Technology Bulletin*, Vol. 4, No. 4, 199–208, 1997.

10. Minchew, B., C. E. Jones, and B. Holt, "Polarimetric analysis of backscatter from the Deepwater Horizon oil spill using L-band synthetic aperture radar," *IEEE Transactions on Geoscience and Remote Sensing*, Vol. 50, No. 10, 3812–3830, 2012.

11. Ding, N. and Z. Min, "An angular cutoff composite model for investigation on electromagnetic scattering from two-dimensional rough sea surfaces," *Chinese Physics B*, Vol. 19, No. 7, 074101, 2010.

12. Awada, A., M. Y. Ayari, A. Khenchaf, and A. Coatanhay, "Bistatic scattering from an anisotropic sea surface: Numerical comparison between the first-order SSA and the TSM models," *Waves in Random and Complex Media*, Vol. 16, No. 3, 383–394, 2006.

13. Voronovich, A. G. and V. U. Zavorotny, "Theoretical model for scattering of radar signals in Ku- and C-bands from a rough sea surface with breaking waves," *Waves in Random Media*, Vol. 11, No. 3, 247–269, 2001.

14. Tsang, L. and J. A. Kong, *Scattering of Electromagnetic Waves*, John Wiley, New York, NY, 1982.

15. Li, J., L.-X. Guo, and H. Zeng, "FDTD investigation on electromagnetic scattering from two-layered rough surfaces under UPML absorbing condition," *Chinese Physics Letters*, Vol. 26, No. 3, 034101, 2009.

16. Zamani, H., A. Tavakoli, and M. Dehmollaian, "Second-order perturbative solution of cross-polarized scattering from multilayered rough surfaces," *IEEE Transactions on Antennas and Propagation*, Vol. 64, No. 5, 1877–1890, 2016.

17. Iodice, A., A. Natale, and D. Riccio, "Kirchhoff scattering from fractal and classical rough surfaces: Physical interpretation," *IEEE Transactions on Antennas and Propagation*, Vol. 61, No. 4, 2156–2163, 2012.

18. Wu, Z. S., J. P. Zhang, L. X. Guo, and P. Zhou, "An improved two-scale model with volume scattering for the dynamic ocean surface," *Progress In Electromagnetics Research*, Vol. 89, 39–56, 2009.

19. Li, J., M. Zhang, P. Wei, and W. Jiang, "An improvement on SSA method for EM scattering from electrically large rough sea surface," *IEEE Geoscience and Remote Sensing Letters*, Vol. 13, No. 8, 1144–1148, 2016.

20. Fung, A. and K. Lee, "A semi-empirical sea-spectrum model for scattering coefficient estimation," *IEEE Journal of Oceanic Engineering*, Vol. 7, No. 4, 166–176, 1982.

21. Lombardini, P. P., B. Fiscella, P. Trivero, and W. D. Garrett, "Modulation of the spectra of short gravity waves by sea surface films: Slick detection and characterization with a microwave probe," *Journal of Atmospheric and Oceanic Technology*, Vol. 6, No. 6, 882–890, 1989.

22. Guo, L.-X., Y.-H. Wang, and Z.-S. Wu, "Application of modified two-scale model for scattering from non-Gaussian sea surface," *Chinese Journal of Radio Science*, Vol. 22, No. 2, 212–218, 2007.

23. Cox, C. and W. Munk, "Measurement of the roughness of the sea surface from photographs of the sun glitter," *Journal of the Optical Society of America A*, Vol. 44, No. 11, 838–850, 1954.